Int. J. Solids Structures Vol. 22, No. 2, pp. 155–169, 1986
Printed in Great Britain.

0020-7683/86 $3.00+.00

FLEXURAL VIBRATION OF SYMMETRICALLY LAMINATED COMPOSITE RECTANGULAR PLATES INCLUDING TRANSVERSE SHEAR EFFECTS

T. J. CRAIG and D. J. DAWE
Department of Civil Engineering, The University of Birmingham, Birmingham B15 2TT, England

(*Received* 20 *January* 1984; *in revised form* 2 *August* 1984; *replacement received* 30 *April* 1985)

Abstract—The flexural vibration of symmetrically laminated rectangular plates is considered, based upon the adoption of a shear-deformation plate theory. This theory is an extension of Mindlin's theory for isotropic plates and includes the effects of both transverse shear deformation and rotary inertia. Two related methods of analysis are described, namely the Rayleigh–Ritz method and the finite-strip method. The assumed displacement fields incorporate the use of the normal modes of vibration of Timoshenko beams and arbitrary combinations of standard plate edge conditions are accommodated. Results presented for orthotropic simply supported plates show very close comparison with available exact results of three-dimensional elasticity theory, when appropriate selection of shear correction factors is made. A range of results is presented for orthotropic square plates with various combinations of boundary conditions, and these results serve to demonstrate both the convergence qualities of the solution procedures and the very large errors that can be associated with analyses based upon the use of the classical plate theory. A final numerical study is concerned with a clamped anisotropic plate and reveals, not unexpectedly, that convergence of results is less rapid than it is for corresponding orthotropic plates.

1. INTRODUCTION

It is becoming widely appreciated nowadays that the useful range of application of classical plate theory (CPT) is quite restricted. For homogeneous isotropic plates, comparisons with the results of three-dimensional elasticity studies for simply supported plates[1–3] reveal that the values of the natural frequencies of flexural vibration as calculated on the basis of CPT can be significantly in error (overestimated) for other than the lowest modes of truly thin plates. The chief source of the error is the neglect of the effect of transverse shear deformation, which is implied by the adoption in CPT of the Kirchhoff assumption that normals to the plate median surface before deformation remain straight and normal to the median surface after deformation. Another source of error in CPT analysis is the neglect of the effect of rotary inertia, though this effect is of considerably less importance than that of transverse shear deformation.

Transverse shear effects are even more pronounced for laminated plates manufactured from orthotropic layers (or laminae or plies) of unidirectional fibrous composite materials, for the reason that the transverse shear modulus of such a plate is usually very small in comparison with the extensional modulus. Laminated plates, with their high strength-to-weight ratios, when fiber materials such as carbon or boron are used, now find extensive employment as structural components, and prediction of their performance is thus of considerable importance. Early analyses of laminated plates were based on CPT, but again, in a similar but more pronounced way to the situation pertaining to isotropic plates, comparisons of the accuracy of such analyses with three-dimensional studes have revealed the large errors that are often associated with the use of CPT: see, for example, [1, 4, 5].

A small number of "improved" or thick-plate theories have been developed which take account of the effect of transverse shear[6]. For homogeneous isotropic materials, a popular one of these is that due to Mindlin[7] in which the basic assumption is that a straight line, originally normal to the plate median surface, is constrained to remain straight but not generally normal to the median surface after deformation: as with CPT, the lateral displacement w does not vary through the plate thickness, while the in-plane displacements vary linearly through the thickness but are not solely proportional to the derivatives of w. In Mindlin plate theory (MPT), because of the inclusion of transverse shear effects, the two cross-sectional rotations ψ_x and ψ_y have to be considered as independent reference quantities, in addition to w. A shear correction factor is introduced to account for the fact that the transverse shear strain distribution is not uniform through the plate thickness. Yang, Norris and Stavsky[8] extended the shear-deformation philosophy of Mindlin to embrace arbitrarily laminated anisotropic plates formed of bonded layers of fiber-reinforced composite material. Whitney and Pagano[9] made some modifications to the theory by using the plane-stress reduced stiffnesses and incorporating shear correction factors into the governing differential equations: they also provided details of static and dynamic applications of the theory for simply supported plates. A study of the approaches of [8] and [9] has been made by Wang and Chou[10], who conclude that the version of the shear-deformation plate theory (SDPT) due to Whitney and Pagano produces somewhat the more accurate results, especially for thick plates.

The thick-plate theory has been shown to produce results which correlate very well with the limited available results of three-dimensional elasticity theory (for simply supported rectangular plates[1–4]), both for isotropic and laminated plates, in problems where it is the overall response of the plate that is of interest, such as in calculating frequencies of vibration or buckling stresses. A proviso attached to this statement is that for laminated plates, the ratio of transverse shear rigidities between one layer and another be not unduly large, else the assumption in SDPT of common angles of cross-sectional rotation through the plate thickness becomes inaccurate. This proviso is met comfortably by most practical laminates, since usually the individual plies are of similar materials. The selection of appropriate shear correction factors is important in applying SDPT[11, 12].

There appear to be relatively few results available which relate to the flexural vibration of rectangular laminated plates when transverse shear and rotary inertia effects are included in the analysis. Among these are closed-form solutions for plates with all edges simply supported[1, 4, 8, 13, 14], approximate single-mode Galerkin method solutions for plates with simply supported and clamped edges[15], a finite-strip solution for the special case of one pair of opposite edges simply supported[16], and finite-element studies[17, 18]. The aim of the present work is to describe the use of two numerical procedures for determining the natural flexural frequencies of a class of laminated rectangular plates, and to present results for some arbitrary combinations of standard support conditions at the plate edges. The SDPT in the form detailed by Whitney and Pagano[9] is used. The numerical procedures are the Rayleigh–Ritz method and one of its piecewise forms, the finite-strip method, and the work is an extension of that described earlier for isotropic plates[19–22], where good accuracy and rate of convergence were demonstrated. The present study is restricted to the popular category of composite plates which are symmetrically laminated with respect to the median surface and, hence, there is no coupling of extensional behavior to bending/transverse shearing behavior. Within this category the plates may be cross-ply or angle-ply laminates and may have orthotropic or anisotropic bending properties. Although only single plates are considered in this paper, it should be realized that the finite-strip method is capable of being extended to apply to the analysis of prismatic plate structures.

2. THE SHEAR-DEFORMATION PLATE THEORY

The basic geometry of the rectangular plate with its coordinates and displacement quantities is shown in Fig. 1. The plate is of uniform thickness h and is composed of a number of layers, each consisting of unidirectional fiber-reinforced composite material. The material of each layer is assumed to possess a plane of elastic symmetry parallel to the xy plane, and axes of material symmetry also exist parallel and normal

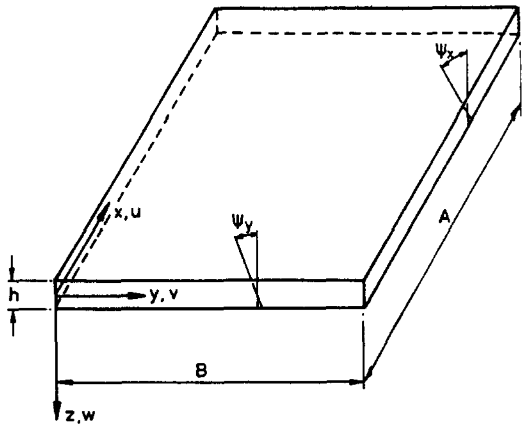

Fig. 1. Plate geometry.

to the fiber direction. In general, of course, the material axes of an individual layer do not coincide with the plate axes.

For plates which are symmetrically laminated with respect to the median surface (the xy plane) there is no bending–stretching coupling, and for flexural vibration within SDPT the displacements u, v and w at a general point in the plate can therefore be assumed to have the form[7, 9]

$$u = z\,\psi_x\,(x, y, t), \qquad v = z\,\psi_y\,(x, y, t), \qquad w = w\,(x, y, t). \tag{1}$$

Here ψ_x and ψ_y are the total rotations along the x and y directions, respectively, of an initially straight vertical line, as indicated in Fig. 1. The constitutive equations for a symmetric laminate consisting of nl orthotropic layers are[9]

$$\begin{Bmatrix} M_x \\ M_y \\ M_{xy} \\ Q_y \\ Q_x \end{Bmatrix} = \begin{bmatrix} D_{11} & & & & \\ D_{12} & D_{22} & & \text{Symmetric} & \\ D_{16} & D_{26} & D_{66} & & \\ 0 & 0 & 0 & A_{44} & \\ 0 & 0 & 0 & A_{45} & A_{55} \end{bmatrix} \begin{Bmatrix} \partial\psi_x/\partial x \\ \partial\psi_y/\partial y \\ \partial\psi_x/\partial y + \partial\psi_y/\partial x \\ \dfrac{\partial w}{\partial y} + \psi_y \\ \dfrac{\partial w}{\partial x} + \psi_x \end{Bmatrix}. \tag{2}$$

Here M_x, M_y and M_{xy} are the bending and twisting moments per unit length, and Q_x and Q_y are the transverse shear forces per unit length. The laminate stiffness coefficients are defined as

$$D_{ij} = \int_{-h/2}^{h/2} Q_{ij}\,z^2\,\mathrm{d}z = \frac{1}{3}\sum_{l=1}^{nl} (Q_{ij})_l\,(h_l^3 - h_{l-1}^3) \qquad (i, j = 1, 2, 6), \tag{3}$$

$$A_{ij} = k_i k_j \int_{-h/2}^{h/2} Q_{ij}\,\mathrm{d}z = k_i k_j \sum_{l=1}^{nl} (Q_{ij})_l\,(h_l - h_{l-1}) \qquad (i, j = 4, 5), \tag{4}$$

where

$$Q_{ij} = C_{ij} - \frac{C_{i3}.C_{3j}}{C_{33}} \qquad (i, j = 1, 2, 6) \tag{5}$$

are the plane-stress reduced-stiffness coefficients, and

$$Q_{ij} = C_{ij} \qquad (i, j = 4, 5) \tag{6}$$

are the shear-stiffness coefficients. The C_{ij} are the stiffness coefficients of three-dimensional elasticity. If the laminate is an orthotropic plate, then D_{16}, D_{26} and A_{45} have zero value, of course.

The coefficients Q_{ij} will vary from layer to layer and for the individual layer l, when the coefficients are $(Q_{ij})_l$, will depend on the material properties and orientation of the layer. In eqns (3) and (4), the quantity h_l is the distance from the median surface to the lower surface of the lth layer. The parameters $k_i k_j$ are shear correction factors, introduced to allow for the fact that the transverse shear strain distributions are not, in fact, uniform through the plate thickness. The selection of appropriate numerical values for these factors is an important, but somewhat contentious, matter: the values are dependent upon the basic material properties of the individual laminae and on the number of laminae forming the plate. Chow[11] derived formulae for evaluating the shear correction factors of orthotropic plates with symmetric lamination, based on the consideration of static cylindrical bending, and Whitney[12] extended this approach to encompass nonsymmetric laminates. The procedure is used here in the calculation of shear correction factors and leads to different values for k_4^2 and k_5^2 for symmetric laminates. Numerical results presented by Noor[23] have demonstrated the suitability of the correction factors determined in the manner suggested by [11] and [12] in predicting the buckling stresses of layered composite plates.

The strain energy per unit area of the plate median surface is

$$\begin{aligned}\Delta U = \tfrac{1}{2}\Bigg[& D_{11}\left(\frac{\partial\psi_x}{\partial x}\right)^2 + D_{22}\left(\frac{\partial\psi_y}{\partial y}\right)^2 + 2D_{12}\frac{\partial\psi_x}{\partial x}\frac{\partial\psi_y}{\partial y} + D_{66}\left(\frac{\partial\psi_x}{\partial y} + \frac{\partial\psi_y}{\partial x}\right)^2 \\ & + 2D_{16}\frac{\partial\psi_x}{\partial x}\left(\frac{\partial\psi_x}{\partial y} + \frac{\partial\psi_y}{\partial x}\right) + 2D_{26}\frac{\partial\psi_y}{\partial y}\left(\frac{\partial\psi_x}{\partial y} + \frac{\partial\psi_y}{\partial x}\right)\Bigg] \\ & + \tfrac{1}{2}\Bigg[A_{44}\left(\psi_y^2 + 2\psi_y\frac{\partial w}{\partial y} + \left(\frac{\partial w}{\partial y}\right)^2\right) + A_{55}\left(\psi_x^2 + 2\psi_x\frac{\partial w}{\partial x} + \left(\frac{\partial w}{\partial x}\right)^2\right) \\ & + 2A_{45}\left(\psi_x\psi_y + \psi_x\frac{\partial w}{\partial y} + \psi_y\frac{\partial w}{\partial x} + \frac{\partial w}{\partial x}\frac{\partial w}{\partial y}\right)\Bigg]\end{aligned} \tag{7}$$

and clearly comprises contributions from both bending and transverse shearing actions.

The kinetic energy per unit area of the plate median surface is

$$\Delta T = \frac{m_1}{2}\left(\frac{\partial w}{\partial t}\right)^2 + \frac{m_2}{2}\left[\left(\frac{\partial\psi_x}{\partial t}\right)^2 + \left(\frac{\partial\psi_y}{\partial t}\right)^2\right]. \tag{8}$$

The quantities m_1 and m_2 depend upon the material density ρ which, in general, varies from layer to layer. Specifically,

$$m_1 = \int_{-h/2}^{h/2} \rho\,dz = \sum_{l=1}^{nl} \rho_l\,(h_l - h_{l-1}) \quad \text{and}$$

$$m_2 = \int_{-h/2}^{h/2} \rho z^2\,dz = \frac{1}{3}\sum_{l=1}^{nl} \rho_l\,(h_l^3 - h_{l-1}^3), \tag{9}$$

where ρ_l is the material density of the lth layer.

In SDPT, three boundary conditions have to be specified at each edge compared to the two of classical theory. In the numerical applications to be presented later, the following "standard" edge conditions are considered on, say, an edge $x = \bar{x}$ (a constant):

simply supported edge (S1 condition) $w = 0, \quad \psi_y = 0, \quad M_x = 0,$ (10)

clamped edge $w = 0, \quad \psi_x = 0, \quad \psi_y = 0,$ (11)

free edge $M_x = 0, \quad M_{yx} = 0, \quad Q_x = 0.$ (12)

3. RAYLEIGH–RITZ ANALYSIS

The Rayleigh–Ritz analysis of homogeneous isotropic rectangular plates, based on the use of MPT, is described fully elsewhere[20]. The approach used in the present work when dealing with composite laminated plates using SDPT is closely related to this earlier work, and so only brief details of the analysis will be recorded here.

In the Rayleigh–Ritz analysis, trial functions are assumed for the three fundamental quantities w, ψ_x and ψ_y over the complete median surface of the plate shown in Fig. 1. Here the form of these functions is taken to be

$$
\begin{aligned}
w(x, y) &= \sum_{n=1}^{r} \sum_{m=1}^{r} a_{mn} W_m(x) W_n(y), \\
\psi_x(x, y) &= \sum_{n=1}^{r} \sum_{m=1}^{r} b_{mn} \Psi_m(x) W_n(y), \qquad (13) \\
\psi_y(x, y) &= \sum_{n=1}^{r} \sum_{m=1}^{r} c_{mn} W_m(x) \Psi_n(y).
\end{aligned}
$$

Equations (13) represent the spatial variation of the fundamental quantities. Of course, in a harmonic vibration at circular frequency p, these quantities also vary sinusoidally with time and, hence, w, ψ_x and ψ_y, as defined in eqns (13), are to be regarded as amplitudes of motion.

In eqns (13), the four unidirectional functions $W_m(x)$, $W_n(y)$, $\Psi_m(x)$ and $\Psi_m(y)$ are the normalized modes of vibration, for lateral deflection and cross-sectional rotation, of Timoshenko beams, having end conditions which are appropriate to the edge conditions of the particular plate under consideration. The form of these beam modes is detailed for isotropic beams in [20]: For the present work, little difference is involved beyond using different values for the physical properties (such as the moduli of elasticity and shear, and the shear correction factor) in the x- and y-directions, as appropriate to the plate under consideration. The quantities a_{mn}, b_{mn} and c_{mn} in eqns (13) are simply generalized displacements, of course.

The Rayleigh–Ritz procedure of the plate vibration problem requires the preliminary generation of solutions for the Timoshenko-beam normalized modes to give the functions $W_m(x)$, etc., for incorporation in the displacement field of eqns (13). This field is then substituted into the expressions for strain energy and kinetic energy per unit plate area, eqns (7) and (8), and integration over the plate median surface gives at any time t the whole-plate strain energy U and kinetic energy T, the latter being proportional to p^2 following the assumption of harmonic motion. The energy quantities U and T also vary sinusoidally with time, of course, but if w, ψ_x and ψ_y in eqns (13) are amplitudes, U and T will have their maximum values U_{max} and T_{max}. In the standard way it is then easy to generate the stiffness matrix $\mathbf{K}$ (obtained from U_{max}) and the consistent mass matrix $\mathbf{M}$ (obtained from T_{max}) and to express the governing set of equations in the usual eigenvalue form

$$(\mathbf{K} - p^2 \mathbf{M}) \mathbf{D} = \mathbf{0}. \qquad (14)$$

The sizes of $\mathbf{K}$ and $\mathbf{M}$ are $3r^2 \times 3r^2$. In eqn (14), $\mathbf{D}$ is the column matrix of all the $3r^2$ generalized displacement amplitudes a_{mn}, b_{mn} and c_{mn}. Equation (14) can be solved using standard procedures to yield the Rayleigh–Ritz-method estimates of natural frequencies and mode shapes of vibration.

4. FINITE-STRIP ANALYSIS

A single thick finite strip is shown in Fig. 2: the strip spans the plate in the x-direction (i.e. the ends of the strip at $x = 0$ and $x = A$ are at the edges of the plate itself), but only spans part of the plate in the y-direction, of course. Over the median surface of an individual strip, the spatial variation of each of the three fundamental quantities is represented as a summation of r products of longitudinal (x-direction) series terms and crosswise (y-direction) polynomial functions. Thus the spatial strip field is

$$\begin{Bmatrix} w \\ \psi_y \\ \psi_x \end{Bmatrix} = \sum_{i=1}^{r} \begin{bmatrix} W_i(x) & 0 & 0 \\ 0 & W_i(x) & 0 \\ 0 & 0 & \Psi_i(x) \end{bmatrix} \begin{bmatrix} \boldsymbol{\phi}_n(y) & \mathbf{0} & \mathbf{0} \\ \mathbf{0} & \boldsymbol{\phi}_n(y) & \mathbf{0} \\ \mathbf{0} & \mathbf{0} & \boldsymbol{\phi}_n(y) \end{bmatrix} \begin{Bmatrix} A_1 \\ A_2 \\ \vdots \\ A_{3n+3} \end{Bmatrix}_i ,$$

or

$$\boldsymbol{\delta} = \sum_{i=1}^{r} \mathbf{s}_i(x)\, \boldsymbol{\alpha}_n(y)\, \mathbf{A}_{ni}. \tag{15}$$

In eqn (15), $\boldsymbol{\phi}_n(y)$, occuring in $\boldsymbol{\alpha}_n(y)$, is a row matrix defined as

$$\boldsymbol{\phi}_n(y) = [1, y, \ldots, y^n], \tag{16}$$

which represents a crosswise polynomial interpolation or order n. The same order of interpolation is assumed for each of the fundamental quantities and, in fact, for all the results presented later a value of $n = 4$ is assumed: neither of these assumptions need be adopted. The column matrix $\mathbf{A}_{ni}$ is the matrix of displacement coefficients corresponding to the ith terms of the longitudinal series. The quantities $W_i(x)$ and $\Psi_i(x)$, occurring in $\mathbf{s}_i(x)$, are the ith terms of the same series of Timoshenko-beam modes used in the Rayleigh–Ritz analysis.

In SDPT only C^0-type continuity is required for each of w, ψ_y and ψ_x, and for the finite strips used here the values of these quantities at $(n + 1)$ reference lines are used as degrees of freedom: for example, with $n = 4$ there are five reference lines—two at the outer edges and three in the interior—as shown in Fig. 2. The displacement coef-

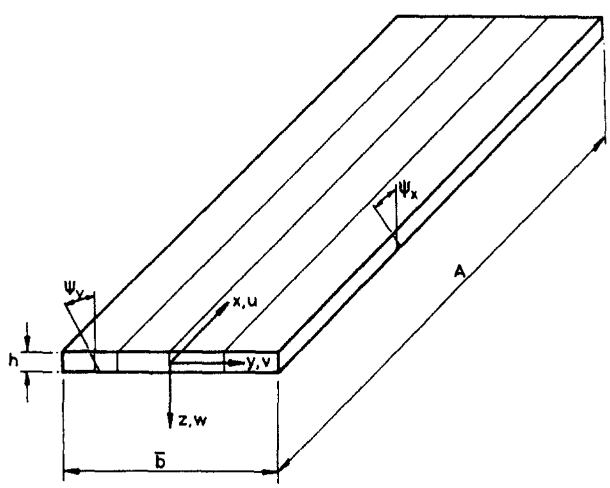

Fig. 2. A finite strip (showing three interior reference lines).

ficients for each series term are easily related to the strip degrees of freedom for the same series term by an equation of the form

$$\mathbf{A}_{ni} = \mathbf{C}_n \, \mathbf{d}_{ni}, \tag{17}$$

where

$$\mathbf{d}_{ni} = \{w_1 \; \psi_{y1} \; \psi_{x1} \; w_2 \cdots \psi_{x(n+1)}\} \tag{18}$$

and $\mathbf{C}_n$ is a square matrix of order $3n + 3$. The spatial variations of w, ψ_x and ψ_y can then be expressed in terms of the strip degrees of freedom by substituting eqn (17) into eqn (15).

In the free-vibration problem it is convenient to regard $\boldsymbol{\delta}$ as representing the amplitudes of w, ψ_x and ψ_y in a harmonic mode and, correspondingly, to work again in terms of the maximum strain energy, $U_{\max}$, and kinetic energy, $T_{\max}$, of the vibrating strip.

Using eqn (7) and integrating over the strip median surface, the maximum strain energy of the strip can be expressed as

$$U_{\max} = \tfrac{1}{2} \int_{-\bar{b}/2}^{\bar{b}/2} \int_0^A (\boldsymbol{\beta}_1^T \mathbf{F}_1 \boldsymbol{\beta}_1 + \boldsymbol{\beta}_2^T \mathbf{F}_2 \boldsymbol{\beta}_2) \, dx \, dy. \tag{19}$$

Here

$$\mathbf{F}_1 = \begin{bmatrix} D_{11} & D_{16} & D_{16} & D_{12} \\ D_{16} & D_{66} & D_{66} & D_{26} \\ D_{16} & D_{66} & D_{66} & D_{26} \\ D_{12} & D_{26} & D_{26} & D_{22} \end{bmatrix}, \tag{20}$$

$$\mathbf{F}_2 = \begin{bmatrix} A_{55} & A_{45} & A_{55} & A_{45} \\ A_{45} & A_{44} & A_{45} & A_{44} \\ A_{55} & A_{45} & A_{55} & A_{45} \\ A_{45} & A_{44} & A_{45} & A_{44} \end{bmatrix}, \tag{21}$$

and

$$\boldsymbol{\beta}_1 = \left\{ \frac{\partial \psi_x}{\partial x} \; \frac{\partial \psi_x}{\partial y} \; \frac{\partial \psi_y}{\partial x} \; \frac{\partial \psi_y}{\partial y} \right\} = \sum_{i=1}^{r} \mathbf{B}_{1i} \, \mathbf{A}_{ni}, \tag{22}$$

$$\boldsymbol{\beta}_2 = \left\{ \psi_x \; \psi_y \; \frac{\partial w}{\partial x} \; \frac{\partial w}{\partial y} \right\} = \sum_{i=1}^{r} \mathbf{B}_{2i} \, \mathbf{A}_{ni}. \tag{23}$$

The matrices $\mathbf{B}_{1i}$ and $\mathbf{B}_{2i}$ can be defined in terms of the beam functions $W_i(x)$ and $\Psi_i(x)$, and the polynomial function $\boldsymbol{\phi}_m(y)$, through use of eqn (15)[21].

The strip strain energy, eqn (19), can be expressed using eqns (17), (22) and (23) as

$$U_{\max} = \tfrac{1}{2} \int_{-\bar{b}/2}^{\bar{b}/2} \int_0^A \left[\sum_{i=1}^{r} \sum_{j=1}^{r} \mathbf{d}_{ni}^T \mathbf{C}_n^T (\mathbf{B}_{1i}^T \mathbf{F}_1 \mathbf{B}_{1j} + \mathbf{B}_{2i}^T \mathbf{F}_2 \mathbf{B}_{2j}) \mathbf{C}_n \mathbf{d}_{nj} \right] dx \, dy. \tag{24}$$

Proceeding further, the strain energy can be put in the familiar form

$$U_{\max} = \tfrac{1}{2} \mathbf{d}_n^T \mathbf{K}_n \mathbf{d}_n, \tag{25}$$

where

$$\mathbf{d}_n = \{\mathbf{d}_{n1} \; \mathbf{d}_{n2} \cdots \mathbf{d}_{ni} \cdots \mathbf{d}_{nr}\} \tag{26}$$

is the column matrix of all the strip freedoms, and $\mathbf{K}_n$ is the strip stiffness matrix, corresponding to crosswise interpolation of order n. This stiffness matrix is of similar form to that defined in more detail in the earlier work[21].

The maximum kinetic energy of the finite strip when vibrating in a harmonic mode having circular frequency p is, making use of eqns (8), (15) and (17),

$$T_{\max} = \tfrac{1}{2} p^2 \int_{-\bar{b}/2}^{\bar{b}/2} \int_0^A \left[\sum_{i=1}^{r} \sum_{j=1}^{r} \mathbf{d}_{ni}^T \, \mathbf{C}_n^T \, \boldsymbol{\alpha}_n^T(y) \, \mathbf{s}_i^T(x) \, \mathbf{G} \, \mathbf{s}_j(x) \, \boldsymbol{\alpha}_n(y) \, \mathbf{C}_n \, \mathbf{d}_{nj} \right] \mathrm{d}x \, \mathrm{d}y, \quad (27)$$

where

$$\mathbf{G} = \begin{bmatrix} m_1 & 0 & 0 \\ 0 & m_2 & 0 \\ 0 & 0 & m_2 \end{bmatrix}. \quad (28)$$

This can be put in the form

$$T_{\max} = \tfrac{1}{2} p^2 \, \mathbf{d}_n^T \, \mathbf{M}_n \, \mathbf{d}_n, \quad (29)$$

where $\mathbf{M}_n$ is the strip consistent mass matrix, which is of similar form to the mass matrix defined in more detail in [21].

The stiffness and mass matrices for the whole plate are obtained by the assembly of strip matrices in the standard manner, and the set of equations governing the plate free-vibration problem then has the same general form as shown for the Rayleigh–Ritz procedure in eqn (14), with $\mathbf{D}$ now interpreted as being the complete column matrix of plate degrees of freedom. The formulation is a consistent one, and exact integration is used in evaluating the strip matrices: hence, as with the use of the Rayleigh–Ritz method, the natural frequencies obtained will be upper bounds to the exact SDPT frequencies.

5. NUMERICAL APPLICATIONS

In this section, results are presented of the application of the two solution procedures described above to laminated plates with a number of combinations of edge conditions and material properties, including orthotropic and anisotropic plates. The plates are in fact all of square planform of side length A, but plates of rectangular planform could just as easily be considered. The plates are described by a symbolism defining the boundary conditions at their four edges; a SCSF plate, for instance, means a plate whose edges are simply supported, clamped, simply supported and free, respectively, starting from the edge $x = 0$ and proceeding clockwise around the plate. Vibrational mode shapes are usually described in the form m, n, where m and n are the numbers of half waves in the x and y directions, respectively.

Except where indicated to the contrary, the values used for the shear correction factors have been those calculated according to the procedures of [11] and [12].

As mentioned earlier, when using the finite-strip method, attention is restricted to the strip model based on quartic crosswise interpolation: each strip, correspondingly, has five reference lines and 15 degrees of freedom per longitudinal series term. Where the number of finite strips is quoted this means the number of strips in the whole plate.

Srinivas and Rao[4] have used three-dimensional elasticity theory to analyze the free vibration of a square simply supported three-layer orthotropic laminate, and their exact results provide very useful benchmark values, with which to compare the predictions of the present methods. Each of the two outer layers of the laminate is of thickness $0.1h$, with the middle layer correspondingly $0.8h$, where h is the total plate

Table 1. Fundamental frequency of SSSS nonhomogeneous orthotropic square plates.

Material ratio $\frac{E_{x1}}{E_{x2}}$	Shear correction factors, $k_4^2 = k_5^2$	Values of $p\sqrt{\rho_2 h^2/E_{x2}}$				
		Three-dimensional elasticity solution [4]	Rayleigh-Ritz solution, r=1	Finite strip solution, 1 strip and r=1	CPT solution [4]	Rayleigh-Ritz solution, r=1, s.c.f.=5/6
1	0.8333	0.04742	0.04740	0.04740	0.04967	0.04740
2	0.7460	0.05704	0.05702	0.05702	0.06058	0.05732
5	0.5324	0.07715	0.07713	0.07713	0.08533	0.07959
10	0.3525	0.09810	0.09806	0.09807	0.11533	0.1065
15	0.2625	0.11203	0.11197	0.11198	0.13899	0.12776

thickness: the thickness-to-side length ratio, h/A, is 0.1. The material properties are those of Aragonite crystals, which are such that for any particular layer.

$$\{Q_{11}\ Q_{12}\ Q_{22}\ Q_{44}\ Q_{55}\ Q_{66}\} = E_x\,\{0.99978\ 0.23119\ 0.52489\ 0.26681\ 0.15991\ 0.26293\},$$

where E_x is the elastic modulus in the x-direction. The laminate is a nonhomogeneous plate with the ratio of the properties of the identical outer layers to those of the central layer (typified by the ratio E_{x1}/E_{x2}, where 1 refers to the outer layers; 2, to the central layer) varying between 1 and 15. The values of the shear correction factors determined according to the procedures of [11] and [12] vary considerably with the material ratio and are recorded in column 2 of Table 1. This table presents results for the fundamental frequency of vibration, based on the predictions of three-dimensional elasticity theory, CPT and SDPT. For the latter plate theory, solutions are presented in columns 4 and 5 of Table 1, corresponding to the use of the Rayleigh–Ritz method (with $r = 1$) and the finite-strip method (with 1 strip and $r = 1$): these solutions are based upon the use of the shear correction factors recorded in column 2 of the table. The SDPT solutions agree to well within 0.1% with the solutions based on three-dimensional elasticity theory, for all the values of material ratio. (It is noted that for this problem, the Rayleigh–Ritz method results are exact within the confines of the adopted SDPT for the prescribed values of the shear corrections factors.) On the other hand the results based on CPT are in considerable error, reaching 24% for a material ratio of 15. The final column of Table 1 lists the results obtained using the present Rayleigh–Ritz procedure, but now with the shear correction factor taken to be 5/6, as is commonly assumed for isotropic materials. These results, while still a considerable improvement on the forecasts of CPT, are markedly inferior at high values of the material ratio to those given in columns 4 and 5 of the table, and this emphasizes the importance of proper selection of shear correction factors.

Now we consider square plates with various edge conditions which are five-layer orthotropic cross-ply laminates, i.e. 0/90/0/90/0 laminates, whose material properties for all plies are identical and correspond to a typical high-modulus-fiber composite with

$$E_L/E_T = 30, \qquad G_{LT}/E_T = 0.6, \qquad G_{TT}/E_T = 0.5$$

and

$$\nu_{LT} = 0.25,$$

where subscripts L and T refer to directions parallel to the fibers and transverse to the fibers, respectively. Two plate thicknesses are considered, with total thickness-to-side length ratios, h/A, of 0.01 and 0.1. The thickness of each of the 0° plies is two-thirds that of each of the 90° plies, so that the total sum of the thicknesses of the 0° plies and

90° plies is the same. The shear correction factors are $k_4^2 = 0.87323$ and $k_5^2 = 0.59139$. The numerical results for these laminates are given in terms of a frequency parameter Ω, which is defined as

$$\Omega = p\frac{A^2}{h}\left[\frac{\rho}{(Q_{11})_t}\right]^{1/2}, \tag{30}$$

where

$$(Q_{11})_t = \sum_{i=1}^{nl}\frac{(Q_{11})_l(h_l - h_{l-1})}{h}, \tag{31}$$

which has the value $0.517745E_L$ for the plate described here.

The manner of convergence of results obtained using the finite-strip method is detailed in Table 2 for the first five natural frequencies of the moderately thick ($h/A = 0.1$) SSSS plate. For this plate the longitudinal series used is exact, and the accuracy of the finite-strip procedure is solely dependent on how closely the crosswise variation of the displacement quantities in a particular mode is represented by the polynomial part of the strip displacement field. The results show that one strip per half wave of crosswise mode shape gives highly accurate results. The Rayleigh–Ritz method again yields results for this problem which are exact within SDPT, and these results are virtually identical with the converged values of the finite-strip approach. Results obtained based on CPT are seen to be in very considerable error. The magnitudes of the percentage differences between the forecasts of SDPT and CPT are very much greater for the present fiber-reinforced laminated plate, with its low transverse shear rigidity, than for the corresponding isotropic plate[19].

In Tables 3 and 4, further detailed results are given, relating to plates with other boundary conditions (viz. SCSC and SSSF) and of both moderately thick ($h/A = 0.1$) and thin ($h/A = 0.01$) geometry. These results are convergence studies for the Rayleigh–Ritz method, plus particular finite-strip method solutions based on the use of three series terms and three strips across the complete plate. These latter results are generated in two separate ways, with the strips running first between an opposite pair of simply supported edges and then running in the direction perpendicular to that. In the tables the quoted CPT solutions are exact within the confines of the classical theory, and were generated using the VIPASA program of Wittrick and Williams[24].

For the SCSC plates there is again very close correspondence between the results of the Rayleigh–Ritz and finite strip methods. For the thin geometry the predictions

Table 2. Frequency parameters Ω for SSSS plate, $h/A = 0.1$, by the finite-strip method.

No. of Strips	No. of series terms, r	Mode 1,1	1,2	2,1	2,2	1,3
1	1	3.604	7.430	-	-	13.495
	2	3.604	7.430	8.838	11.023	13.495
2	1	3.604	7.094	-	-	11.763
	2	3.604	7.094	8.838	10.799	11.763
3	1	3.604	7.093	-	-	11.715
	2	3.604	7.093	8.838	10.799	11.715
SDPT exact solution (Rayleigh-Ritz method)		3.604	7.093	8.838	10.799	11.714
CPT solution		4.214	9.829	13.840	16.854	20.646

Table 3. Frequency parameters Ω for SCSC plates, h/A = 0.1 and 0.01 (RRM denotes Rayleigh–Ritz method, FSM denotes finite-strip method).

$\frac{h}{A}$	Solution Procedure		Mode 1,1	1,2	2,1	2,2	1,3
0.1	RRM solution	r=1	4.490	-	-	-	-
		r=2	4.490	7.912	9.214	11.328	-
		r=3	4.489	7.912	9.214	11.328	12.202
		r=4	4.489	7.911	9.214	11.328	12.202
		r=5	4.489	7.911	9.213	11.328	12.202
	FSM solution	SS series	4.489	7.910	9.213	11.327	12.203
		CC series	4.489	7.912	9.213	11.328	12.203
	CPT solution		6.215	14.553	14.612	20.055	27.747
0.01	RRM solution	r=1	6.184	-	-	-	-
		r=2	6.184	14.369	14.502	19.829	-
		r=3	6.184	14.369	14.500	19.829	27.134
		r=4	6.184	14.369	14.500	19.829	27.134
		r=5	6.184	14.369	14.500	19.828	27.134
	FSM solution	SS series	6.184	14.382	14.500	19.835	27.168
		CC series	6.184	14.369	14.502	19.830	27.133
	CPT solution		6.215	14.553	14.612	20.055	27.747

Table 4. Frequency parameters Ω for SSSF plates, h/A = 0.1 and 0.01.

$\frac{h}{A}$	Solution Procedure		Mode 1,1	1,2	2,1	2,2	1,3
0.1	RRM solution	r=1	2.909	-	-	-	-
		r=2	2.908	4.405	8.543	9.260	-
		r=3	2.908	4.404	8.543	9.257	8.516
		r=4	2.908	4.403	8.542	9.256	8.515
		r=5	2.908	4.402	8.542	9.255	8.515
	FSM solution	SS Series	2.907	4.396	8.541	9.249	8.510
		SF Series	2.908	4.403	8.543	9.257	8.517
	CPT Solution		3.414	5.208	13.490	14.400	12.183
0.01	RRM solution	r=1	3.409	-	-	-	-
		r=2	3.408	5.200	13.390	14.307	-
		r=3	3.408	5.198	13.390	14.297	12.118
		r=4	3.408	5.197	13.390	14.295	12.118
		r=5	3.408	5.197	13.390	14.294	12.117
	FSM solution	SS Series	3.408	5.197	13.389	14.294	12.125
		SF Series	3.408	5.197	13.392	14.299	12.118
	CPT Solution		3.414	5.208	13.490	14.400	12.183

of CPT are slightly high as expected, while for the moderately thick plate, the neglect of transverse shear and rotary inertia leads to very large overestimates of the natural frequencies, reaching 127% for mode (1, 3). For the SSSF plates, there is also very good agreement between the results of the different methods. It is recalled from earlier work on isotropic plates[21, 22] that when longitudinal series are used which incorporate a free-end condition, there is some effect on the kinematic admissibility of the plate displacement field. This effect will apply to the present Rayleigh–Ritz method solutions and to the finite-strip method solutions when using the SF series, but not when using the SS series. In fact, the practical influence of the effect on numerical values is tiny, as is evidenced by the closeness of all three types of SDPT result in Table 4. The predictions of CPT for the moderately thick SSSF plate are again seen to be very considerable overestimates.

Results for the moderately thick CCCC plate are recorded in Table 5. Details of the convergence of the results of both the finite-strip and Rayleigh–Ritz methods are given. It is seen that there is almost exact correspondence between the most accurate (i.e. lowest) values obtained for each solution procedure, and this provides a good check on their validity. No other independent comparative solutions are available for this particular plate, whether based on SDPT or CPT.

Although series terms up to the level $r = 5$ have been used when applying the Rayleigh–Ritz method in the above studies of orthotropic plates, it is clear that in the class of problem considered here, an accurate value for the fundamental frequency is obtained with the use of only the minimal displacement field, corresponding to $r = 1$. Also, when applying the finite-strip method it is usually sufficient for practical purposes to use only a single strip (in the whole plate) and a single series term (for each of the fundamental quantities) in calculating the fundamental frequency.

Table 5. Frequency parameters Ω for CCCC plate, $h/A = 0.1$.

		No. of series terms, r	Mode 1,1	1,2	2,1	2,2	1,3
Finite strip method solution	1 strip	1	5.640	9.102	-	-	14.628
		2	5.640	9.102	9.972	12.304	14.628
		3	5.639	9.102	9.972	12.304	14.628
		4	5.638	9.102	9.972	12.303	14.628
		5	5.638	9.101	9.972	12.303	14.627
	2 strips	1	5.638	8.583	-	-	12.678
		2	5.638	8.583	9.971	11.931	12.678
		3	5.637	8.582	9.971	11.931	12.678
		4	5.637	8.582	9.971	11.931	12.678
		5	5.636	8.581	9.971	11.931	12.677
	3 strips	1	5.638	8.582	-	-	12.628
		2	5.638	8.582	9.971	11.930	12.628
		3	5.637	8.581	9.971	11.930	12.628
Rayleigh-Ritz method solution		1	5.786	-	-	-	-
		2	5.638	8.583	9.972	11.932	-
		3	5.638	8.583	9.971	11.932	12.627
		4	5.638	8.582	9.971	11.931	12.627
		5	5.637	8.582	9.971	11.931	12.627

The final numerical study concerns the vibration of a fully clamped square anisotropic plate, with bending–twisting coupling present and D_{16} and D_{26} correspondingly non-zero. The plate in question is one that has been analyzed within the framework of CPT by Ashton and Whitney[25]: it is a single-layer plate of orthotropic material, but the principal axes of orthotropy are orientated at an angle of 30° to the x axis. The material properties of the orthotropic layer are

$$E_L/E_T = 10, \qquad G_{LT}/E_T = G_{TT}/G_T = 0.25, \qquad \nu_{LT} = 0.3.$$

Here two plate thicknesses are investigated, these being $h/A = 0.01$ and 0.1 again, and the finite-strip method is used to calculate the first four frequencies in each case. The shear correction factors are taken to be $k_4^2 = k_5^2 = 5/6$: these are the values calculated according to the procedures of [11] and [12] for an equivalent orthotropic plate (i.e. for the plate as defined here, except that $D_{16} = D_{26} = 0$). Results are presented in Table 6, and it is apparent that convergence is poorer for the anisotropic plates than for orthotropic plates, particularly with regard to increase in the value of r. This reduction in efficiency of solution is due to the fact that the nodal lines of the vibrational mode shapes are highly skewed for the anisotropic plates. Nevertheless, it appears from the manner of convergence of the results that the quoted values of frequency corresponding to the use of three strips and $r = 6$ are probably within a percent or so of the exact frequencies within SDPT. For the thicker geometry, the differences between the calculated SDPT and CPT frequencies indicate, once more, the very significant influence of transverse shear and rotary interia. Incidentally, the comparative CPT results are based on the use of the Rayleigh–Ritz method and Ashton and Whitney[25] note that convergence of their approximate results is much slower for anisotropic plates than for orthotropic plates.

6. CONCLUSIONS

The flexural vibration of rectangular laminated plates, manufactured from layers of unidirectional fibrous composite material, has been studied, based upon the use of

Table 6. Frequencies of CCCC anisotropic plates by the finite-strip method.

No. of strips	No. of series terms, r	Values of $p\frac{A^2}{h}\left[\frac{12(1-\nu_{LT}\nu_{TL})}{E_L}\right]^{\frac{1}{2}}$							
		$h/A = 0.1$				$h/A = 0.01$			
		Mode 1	Mode 2	Mode 3	Mode 4	Mode 1	Mode 2	Mode 3	Mode 4
2	1	15.74	24.72	36.73	53.04	23.34	38.98	63.85	125.57
	2	14.70	22.90	28.89	33.46	21.59	34.11	55.24	55.55
	3	14.50	22.50	27.24	31.57	21.39	33.49	52.40	52.92
	4	14.39	22.40	26.98	31.33	21.34	33.46	51.70	52.72
	5	14.32	22.29	26.74	31.13	21.31	33.38	51.59	52.62
	6	14.28	22.25	26.65	31.07	21.30	33.38	51.51	52.59
3	1	15.74	24.71	36.46	50.10	23.32	38.95	62.15	93.78
	2	14.70	22.89	28.89	33.32	21.52	33.81	53.41	54.86
	3	14.50	22.48	27.24	31.50	21.31	33.12	50.76	52.07
	4	14.39	22.39	26.97	31.27	21.26	33.09	50.57	51.41
	5	14.31	22.27	26.73	31.07	21.23	33.01	50.47	51.29
	6	14.28	22.24	26.64	31.01	21.22	33.00	50.43	51.21
CPT solution[25]		21.35	33.18	50.72	51.87	21.35	33.18	50.72	51.87

shear-deformation plate theory. Two numerical techniques have been employed in the study, viz. the Rayleigh–Ritz method and the finite-strip method, and in both the trial displacement functions make use of the normal modes of vibration of Timoshenko beams. Boundary conditions at the plate edges can be any combination of the standard types.

For orthotropic plates the Rayleigh–Ritz method is very efficient, being capable of accurately predicting the frequency of the fundamental mode of vibration using just a one-term representation of each of the three basic reference quantities. The finite-strip method has also been shown to be an accurate analysis technique, with good convergence properties: this method has the significant virtue that it can be extended to deal with longitudinally invariant plate structures, rather than with just single plates as described herein. Where comparison can be made with three-dimensional elasticity solutions—for plates with all edges simply supported—it has been shown that there is very close correspondence between the present results based on SDPT and the elasticity theory results, provided that appropriate shear correction factors are used in the shear-deformation approach. For more-general boundary conditions, comparative solutions (other than those based on the classical plate theory) are not available, but the fact that the two solution procedures yield converged frequency predictions that are very close to one another, and that their convergence qualities are good, provides strong evidence of their validity.

For anisotropic plates some loss of accuracy is involved, which is to be expected since the mode shapes of vibration become more complicated. Nevertheless, convergence to true SDPT solutions will occur with use of the two subject methods, albeit at reduced rate.

The scale of the influence of transverse shear, and of rotary inertia, depends on the particular application, but increases with increase in the ratio of plate thickness to half wavelength of vibration, with increase in the degree of constraint imposed at the plate edges and, of course, with increase in the transverse shear flexibility of the plate material. Use of an analysis based on the classical plate theory can often lead to unacceptable errors for other than the lowest modes of vibration of very thin plates.

Acknowledgements—One of the authors (T.J.C.) is grateful for the financial support of the Science and Engineering Research Council and the Royal Aircraft Establishment, Farnborough, England, during the period of the investigation reported in this paper.

REFERENCES

1. S. Srinivas, C. V. Joga Rao and A. K. Rao, An exact analysis for vibration of simply supported homogeneous and laminated thick rectangular plates. *J. Sound Vib.* **12**, 187–199 (1970).
2. Y. C. Lee and H. Reismann, Dynamic of rectangular plates. *Int. J. Eng. Sci.* **7**, 93–113 (1969).
3. K. T. Sundara Raja Iyengar and P. V. Raman, Free vibration of rectangular plates of arbitrary thickness. *J. Sound Vib.* **54**, 229–236 (1977).
4. S. Srinivas and A. K. Rao, Bending, vibration and buckling of simply supported thick orthotropic rectangular plates and laminates. *Int. J. Solids Structures* **6**, 1463–1481 (1970).
5. N. J. Pagano, Exact solutions for rectangular bidirectional composites and sandwich plates. *J. Compos. Mater.* **4**, 20–36 (1970).
6. C. W. Bert, Analysis of plates. In *Structural Design and Analysis—I* (Edited by C. C. Chamis), Chap. 4. Academic, New York (1974).
7. R. D. Mindlin, Influence of rotary inertia and shear on flexural motions of isotropic elastic plates. *J. Appl. Mech.* **18**, 31–38 (1951).
8. P. C. Yang, C. H. Norris and Y. Stavsky, Elastic wave propagation in heterogeneous plates. *Int. J. Solids Structures* **2**, 665–684 (1966).
9. J. M. Whitney and N. J. Pagano, Shear deformation in heterogeneous anisotropic plates. *J. Appl. Mech.* **37**, 1031–1036 (1970).
10. A. S. O. Wang and P. C. Chou, A comparison of two laminated plate theories. *J. Appl. Mech.* **39**, 611–613 (1972).
11. T. S. Chow, On the propagation of flexural waves in an orthotropic laminated plate and its response to an impulsive load. *J. Compos. Mater.* **5**, 306–319 (1971).
12. J. M. Whitney, Shear correction factors for orthotropic laminates under static load. *J. Appl. Mech.* **40**, 302–304 (1973).
13. C. W. Bert and T. L. C. Chen, Effect of shear deformation on vibration of antisymmetric angle-ply laminated rectangular plates. *Comput. Struct.* **14**, 465–473 (1978).

14. A. K. Noor, Free vibration of multilayered composite plates. *AIAA J.* **11**, 1038–1039 (1973).
15. M. Sathyamoorthy and C. Y. Chia, Nonlinear vibration of anisotropic rectangular plates including shear and rotatory inertia. *Fibre Sci. Technol.* **13**, 337–361 (1980).
16. E. Hinton, A note on a thick finite-strip method for the free vibration of laminated plates. *Earthquake Eng. Struct. Dyn.* **4**, 511–514 (1976).
17. J. N. Reddy, Free vibration of antisymmetric angle-ply laminated plates including transverse shear deformation by the finite-element method. *J. Sound Vib.* **66**, 565–576 (1979).
18. J. N. Reddy, Finite-element modeling of layered anisotropic composite plates and shells: a review of recent research. *Shock Vib. Dig.* **13**, 3–14 (1981).
19. D. J. Dawe, Finite-strip models for vibration of Mindlin plates. *J. Sound Vib.* **59**, 441–452 (1978).
20. D. J. Dawe and O. L. Roufaeil, Rayleigh–Ritz vibration analysis of Mindlin plates. *J. Sound Vib.* **69**, 345–359 (1980).
21. O. L. Roufaeil and D. J. Dawe, Vibration analysis of rectangular Mindlin plates by the finite-strip method. *Comput. Struct.* **12**, 833–842 (1980).
22. O. L. Roufaeil and D. J. Dawe, Rayleigh–Ritz vibration analysis of rectangular Mindlin plates subjected to membrane stresses. *J. Sound Vib.* **85**, 263–275 (1982).
23. A. K. Noor, Stability of multilayered composite plates. *Fibre Sci. Technol.* **8**, 81–89 (1975).
24. W. H. Wittrick and F. W. Williams, Buckling and vibration of anisotropic or isotropic plate assemblies under combined loadings. *Int. J. Mech. Sci.* **16**, 209–239 (1974).
25. J. E. Ashton and J. M. Whitney, *Theory of Laminated Plates* (Section 5.8). Technomic, Stanford (1970).